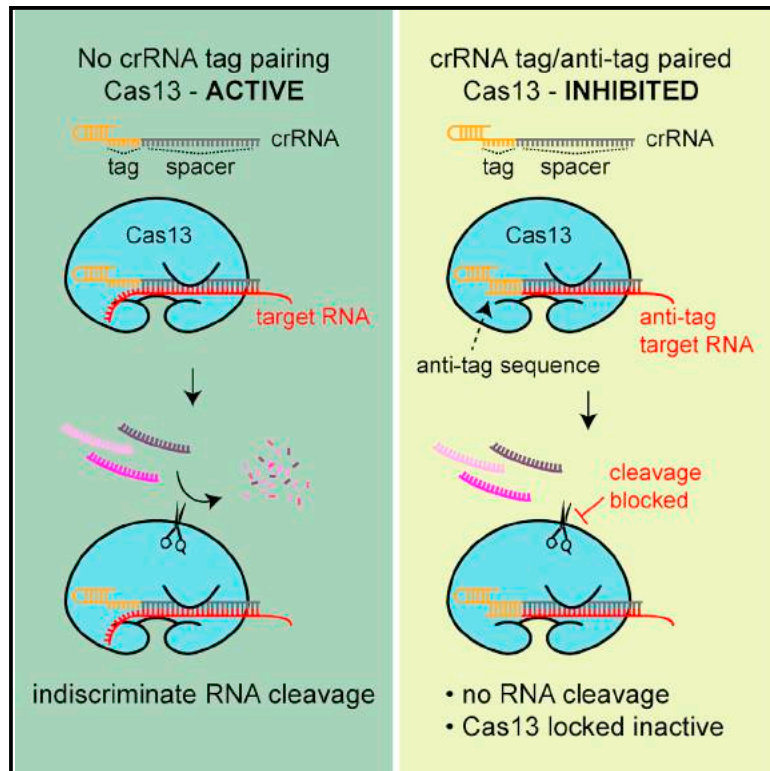


Molecular Cell

RNA Guide Complementarity Prevents Self-Targeting in Type VI CRISPR Systems

Graphical Abstract



Authors

Alexander J. Meeske,
Luciano A. Marraffini

Correspondence

marraffini@rockefeller.edu

In Brief

Type VI CRISPR systems use the RNA-guided Cas13 nuclease to sense and cleave infecting RNA targets. Meeske et al. show that prevention of autoimmunity is mediated by sensing of extended complementarity between the Cas13 RNA guide and target RNAs that may originate from the CRISPR locus.

Highlights

- Target-activated Cas13 cleaves RNA indiscriminately in its native bacterial host
- Extended complementarity between guide and target RNA blocks cleavage
- Targets with extended guide pairing lock Cas13 into an inhibited state
- Inhibition by extended complementarity prevents self-targeting

RNA Guide Complementarity Prevents Self-Targeting in Type VI CRISPR Systems

Alexander J. Meeske¹ and Luciano A. Marraffini^{1,2,*}

¹Laboratory of Bacteriology, The Rockefeller University, 1230 York Avenue, New York, NY 10065, USA

²Lead Contact

*Correspondence: marraffini@rockefeller.edu

<https://doi.org/10.1016/j.molcel.2018.07.013>

SUMMARY

All immune systems use precise target recognition to interrogate foreign invaders. During CRISPR-Cas immunity, prokaryotes capture short spacer sequences from infecting viruses and insert them into the CRISPR array. Transcription and processing of the CRISPR locus generate small RNAs containing the spacer and repeat sequences that guide Cas nucleases to cleave a complementary protospacer in the invading nucleic acids. In most CRISPR systems, sequences flanking the protospacer drastically affect cleavage. Here, we investigated the target requirements of the recently discovered RNA-targeting type VI-A CRISPR-Cas system in its natural host, *Listeria seeligeri*. We discovered that target RNAs with extended complementarity between the protospacer flanking sequence and the repeat sequence of the guide RNA are not cleaved by the type VI-A nuclease Cas13, neither *in vivo* nor *in vitro*. These findings establish fundamental rules for the design of Cas13-based technologies and provide a mechanism for preventing self-targeting in type VI-A systems.

INTRODUCTION

Immune systems protect their host by specifically detecting and eliminating foreign agents. To achieve this, an efficient immune response must make use of precise target recognition mechanisms. CRISPR systems and their associated (Cas) proteins defend their prokaryotic hosts from invasion by bacteriophage (Barrangou et al., 2007) and plasmids (Marraffini and Sontheimer, 2008). Immunological memories of infection by these genetic elements are captured and preserved by CRISPR systems in an array of short (~30 nt) segments of foreign DNA called spacers, which are flanked by repeat sequences on either side (Barrangou et al., 2007). The array is transcribed as a long precursor CRISPR RNA (pre-crRNA) and then cleaved at each repeat sequence to liberate individual CRISPR RNAs (crRNAs) (Brouns et al., 2008; Deltcheva et al., 2011; Hale et al., 2008). These are small RNAs that contain the spacer sequence and a short region of the repeat, known as the crRNA tag. After processing, crRNAs form a ribonucleoprotein complex with Cas

effector nucleases and guide them to destroy foreign nucleic acid targets (called protospacers) that are complementary to the spacer region.

A wide variety of CRISPR-Cas systems have been discovered and categorized into six types on the basis of their cas gene content and mechanism of target interference (Makarova et al., 2015; Shmakov et al., 2017). In all CRISPR types studied to date, the sequences that flank the protospacer are fundamental for target recognition and for the prevention of an immune reaction against the spacer sequences in the CRISPR array itself. In the DNA-targeting type I, II, and V CRISPR-Cas systems, the presence of a short protospacer adjacent motif (PAM) is strictly required for target recognition and cleavage (Deveau et al., 2008; Gasiunas et al., 2012; Jinek et al., 2012; Semenova et al., 2011; Zetsche et al., 2015). Importantly, PAMs are absent from the repeats that flank the spacer in the CRISPR array of these systems, preventing autoimmune cleavage of these targets that are complementary to the crRNA guide and reside within the host genome. In contrast, type III CRISPR systems are much more flexible in their protospacer-flanking sequence requirements for cleavage: most flanking sequences license targeting, except those having high levels of homology to the CRISPR repeat (Elmore et al., 2016; Marraffini and Sontheimer, 2010; Pyenson et al., 2017). Type III CRISPR-Cas systems are unique in that they use the crRNA guide to sense target transcripts and cleave both DNA and RNA (Elmore et al., 2016; Estrella et al., 2016; Kazlauskienė et al., 2016; Samai et al., 2015). Targets with complementarity extending beyond the spacer-protospacer RNA duplex into the crRNA tag region fail to activate the DNase activity of Cas10 within the type III effector ribonucleoprotein complex (Elmore et al., 2016; Estrella et al., 2016; Kazlauskienė et al., 2016; Samai et al., 2015). It is believed that this targeting rule protects the CRISPR locus from self-cleavage upon antisense transcription of the array (Kazlauskienė et al., 2016; Lillestøl et al., 2009).

Type VI-A CRISPR systems encode a large single effector protein called Cas13, which binds to RNA targets in a crRNA-guided manner (Abudayyeh et al., 2016; East-Seletsky et al., 2016; Liu et al., 2017a). Once target bound, Cas13 undergoes a conformational change, unleashing a nonspecific *trans*-RNA cleavage activity catalyzed by its dual higher eukaryotes and prokaryotes nucleotide-binding (HEPN) domains. Here, we investigated the targeting rules used by Cas13 in *Listeria seeligeri*, a natural host of the type VI-A CRISPR-Cas system. A previous report that investigated the function of the *Leptotrichia shahii* type VI-A system via overexpression of this locus in an *Escherichia*

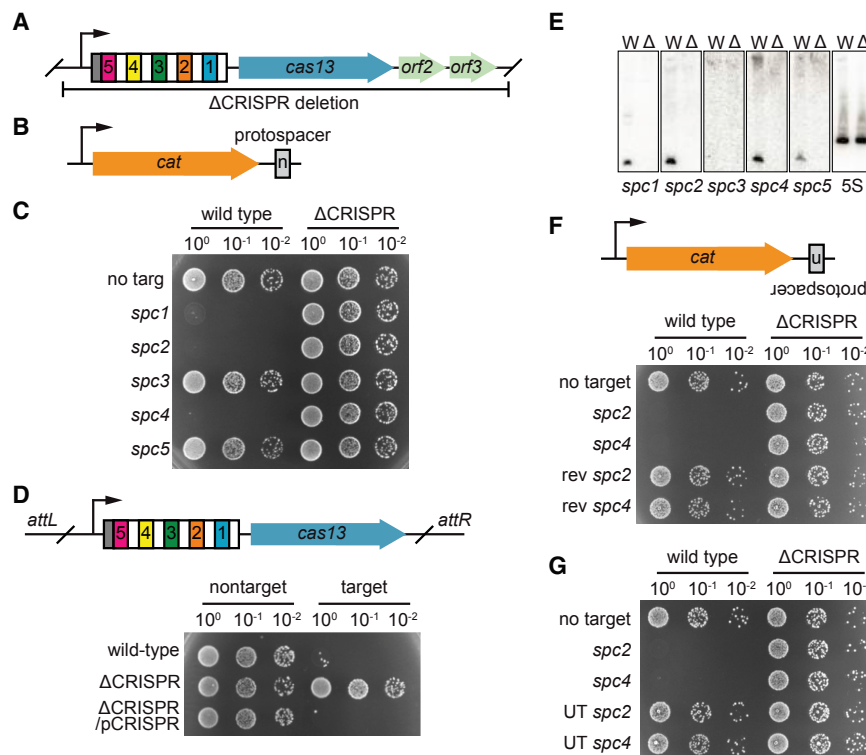


Figure 1. The *Listeria seeligeri* Type VI-A CRISPR System Restricts Conjugative Plasmid Transfer

(A) Schematic of *L. seeligeri* type VI CRISPR locus and region deleted for this study, with spacers shown in colors and repeats shown in white. Degenerate repeat is indicated in gray. (B) Schematic of pTarget plasmid constructs with a protospacer inserted into the coding strand of the *cat* gene 3' UTR. (C) Conjugation assay for CRISPR interference. Wild-type or Δ CRISPR *L. seeligeri* recipients were co-cultured with an *E. coli* donor containing a CRISPR target matching the indicated spacer. Transconjugants were selected from diluted cultures on media containing nalidixic acid and chloramphenicol. (D) Complementation of CRISPR locus deletion by ectopically integrated pCRISPR construct. (E) Northern blots with probes against each spacer in the CRISPR array and 5S rRNA loading control. (F and G) Lack of targeting against protospacers in reverse orientation (F) or placed in untranscribed (UT) regions (G). See also Figure S1.

coli heterologous host indicated that Cas13 recognizes a single nucleotide motif adjacent to the target called the protospacer flanking site (PFS) (Abudayyeh et al., 2016), yet another study reported no PFS rules for Cas13 targeting *in vitro* (East-Seletsky et al., 2016). Our *in vivo* and *in vitro* data indicate that, similar to the mechanism used by type III CRISPR systems, extended complementarity between the crRNA tag and the target flanking sequence (the “anti-tag”) blocks the activation of Cas13, preventing RNA cleavage. We determined that at least 7 nt of the anti-tag contribute to target discrimination and that complementarity at these sites is necessary and sufficient for target protection. Our results show that, similar to type III systems, type VI-A systems can use tag:anti-tag RNA pairing to protect the host from toxic Cas13 misactivation by antisense transcription of the CRISPR locus. Furthermore, we found that anti-tag RNAs act as potent inhibitors of Cas13 activity, suggesting a potential regulatory mechanism for this system. Our findings also establish important targeting rules for Cas13-based diagnostics and RNA knockdown technologies (Abudayyeh et al., 2017; East-Seletsky et al., 2016; Gootenberg et al., 2017, 2018; Myhrvold et al., 2018).

RESULTS

The *Listeria seeligeri* Type VI-A CRISPR System Restricts Conjugative Plasmid Transfer

To study type VI-A CRISPR function under conditions that most accurately approximate those in nature, we performed experiments in *Listeria seeligeri*. Its 2.8-Mb genome contains a type VI-A CRISPR system with five endogenous spacers alongside

a *cas13* homolog (Figure 1A). The CRISPR array begins in an unusual orientation, with a degenerate repeat at the 5' end preceding the spacers. Degenerate repeats are commonly observed at one end of a CRISPR array and flank the oldest, often nonfunctional spacers; therefore, we hypothesized that the newest spacers are located at the 3' end and began our spacer nomenclature at this end of the array (Makarova et al., 2015). We developed a “loop-in, loop-out” allelic replacement method for *L. seeligeri* and constructed a deletion of the CRISPR locus (STAR Methods; Figure S1A), including *cas13* and two neighboring open reading frames (ORFs) predicted to be in the same operon. Using the *E. coli*-*Listeria* shuttle vector pAM8, we engineered pTarget conjugative plasmids, each containing a protospacer complementary to one of the endogenous *L. seeligeri* spacers inserted into the 3' UTR of the chloramphenicol acetyltransferase (*cat*) gene (Figure 1B). Each pTarget plasmid was transferred into wild-type and Δ CRISPR recipient strains via conjugative mating with an *E. coli* donor, and transconjugants were isolated using a combination of nalidixic acid to kill donors and chloramphenicol to select for pTarget (Figure 1C). All target plasmids gave rise to *L. seeligeri* transconjugants with the Δ CRISPR recipient, as did a control plasmid lacking a target sequence when mated with a wild-type recipient. Conjugation of plasmids harboring targets matching *spc1*, *spc2*, and *spc4* was restricted in wild-type, but not Δ CRISPR, cells, likely due to cleavage of the *cat* transcript. Re-incorporation of the CRISPR-Cas locus (including the CRISPR array and *cas13* but not *orf2* or *orf3*) into the PSA phage integration site of Δ CRISPR bacteria using the pPL2e vector (Lauer et al., 2002) restored CRISPR targeting of the conjugative plasmid carrying the *spc2* protospacer, confirming CRISPR-dependent, anti-conjugation immunity (Figure 1D). To

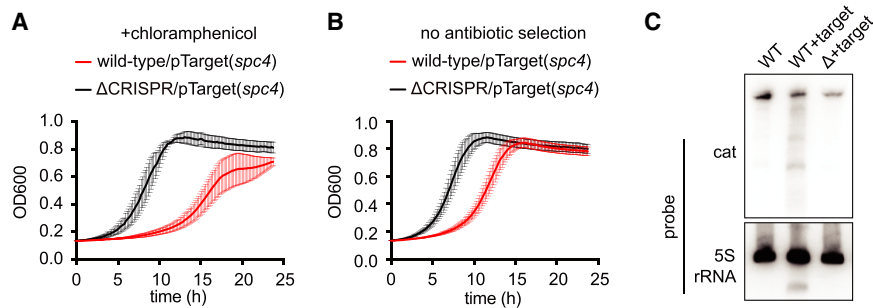


Figure 2. The Type VI CRISPR System Elicits Collateral RNA Cleavage in the Native Host

(A and B) Liquid growth assays of the indicated strains illustrating CRISPR-dependent growth defects in the presence of target with (A) or without (B) target selection. Error bars represent SEM from four biological replicates. OD600, optical density 600.

(C) Northern blot analysis of target (*cat*) and nontarget (5S rRNA) transcripts in the indicated strains. WT, wild-type.

investigate the lack of restriction of plasmids containing targets matching *spc3* or *spc5*, we looked for the presence of mature, matching crRNAs by northern blot (Figure 1E). For all the functional spacers (*spc1*, *spc2*, and *spc4*), crRNAs of the expected length (55 nt) were detected in wild-type, but not in Δ CRISPR hosts. crRNAs matching *spc3* were undetectable, suggesting that this spacer is not functional due to lack of processing or instability of its crRNA. In contrast, *spc5* crRNAs were expressed at levels similar to the other, functional crRNAs; therefore, we speculate that the resulting crRNA may not be competent for interference due to the presence of the degenerate repeat.

Consistent with the reported RNA-targeting mechanism of other type VI CRISPR systems (Abudayyeh et al., 2016), the transfer of plasmids with protospacers inserted in the non-transcribed strand of the *cat* gene (Figures 1F and S1B), as well as the conjugation of plasmids with targets inserted into a weakly transcribed region of pTarget (Figures 1G and S1B), was not restricted. *In vitro* experiments with purified Cas13 have demonstrated that it catalyzes nonspecific “collateral” RNase activity upon target binding (Abudayyeh et al., 2016; East-Seletsky et al., 2016; Liu et al., 2017b). Furthermore, it was reported that *Leptotrichia shahii* Cas13 activity elicited a growth defect when expressed in *E. coli* along with a target RNA (Abudayyeh et al., 2016). However, Cas13 achieves specific RNA knockdown in mammalian cells without apparent collateral activity (Abudayyeh et al., 2017). We noticed the formation of very small transconjugant colonies several days after of conjugation of the *spc4* pTarget plasmid into wild-type recipients. We confirmed this severe growth defect by measuring the growth of wild-type and Δ CRISPR transconjugants in liquid cultures in the presence of chloramphenicol (Figure 2A). To investigate the contribution of collateral RNA damage to this growth defect, we repeated the experiment in the absence of chloramphenicol, where the knockdown of the *cat* transcript target should not have an effect on cell growth. Again, we observed a marked growth defect of wild-type transconjugants (Figure 2B), consistent with the observed nonspecific RNA cleavage activity in other type VI CRISPR systems and demonstrating that collateral RNase activity also occurs in natural hosts. Finally, we performed northern blots to detect the *cat* target transcript and a control 5S rRNA in the slow-growing, wild-type transconjugants (Figure 2C). Consistent with the presence of both specific and non-specific Cas13-mediated RNA degradation, we observed cleavage products for both transcripts, which were absent from wild-type cells carrying a targetless plasmid and from Δ CRISPR transconjugant

samples. Altogether, these data show that, in *L. seeligeri*, a native host, type VI-A CRISPR-Cas systems provide immunity against plasmid conjugation through the degradation of both spacer-specific and unrelated transcripts, the latter resulting in a severe growth defect of the host.

A GTT Sequence Immediately Downstream of the Target Protospacer Enables Escape from Type VI-A CRISPR Targeting

Previous studies in which type VI-A CRISPR systems were over-expressed in a heterologous host have uncovered sequence motifs adjacent to the target RNA protospacer that are required for the activation of Cas13 interference activity *in vivo* (Abudayyeh et al., 2016, 2017; Cox et al., 2017; East-Seletsky et al., 2016; Liu et al., 2017b). This motif (referred to as the PFS) is typically found at one end of the RNA protospacer and, in the case of type VI-A systems, consists of a preference for non-G at the +1 position following the 3' end of the target. In contrast, other reports of Cas13a RNA cleavage activity *in vitro* did not detect any sequence preference at the PFS position (East-Seletsky et al., 2016). Similarly flexible target flanking sequence requirements were reported for other variants of Cas13 (Abudayyeh et al., 2016; Cox et al., 2017; Konermann et al., 2018; Liu et al., 2017b; Yan et al., 2018). Therefore, we wondered whether the PFS or other target sequence preferences of Cas13 in its native host might differ from those observed in transplanted systems.

To probe PFS requirements, we built target (*spc2* and *spc4*) plasmid libraries containing five randomized nucleotides (1,024 different sequences) on either the 5' or the 3' side of the protospacer sequence following the *cat* gene and transformed the libraries by conjugation separately into wild-type and Δ CRISPR *L. seeligeri*, selecting for target expression (Figure S2A). For each combination of library and recipient strain, 20,000 transformants were pooled, target plasmids were isolated, the target site was amplified by PCR, and the products were subjected to next-generation sequencing. In this experiment, the abundance of flanking sequences that escape targeting would be enriched in the wild-type strain but unaffected in the Δ CRISPR strain; thus, we calculated the enrichment ratio for each PFS as wild-type/ Δ CRISPR reads. Upon conjugation into the Δ CRISPR strain, both libraries yielded mostly large colonies. In contrast, transconjugants of the wild-type strain were heterogeneous with both small and large colonies. When we tabulated PFS representation in the Δ CRISPR strain, each of the 1,024 possible

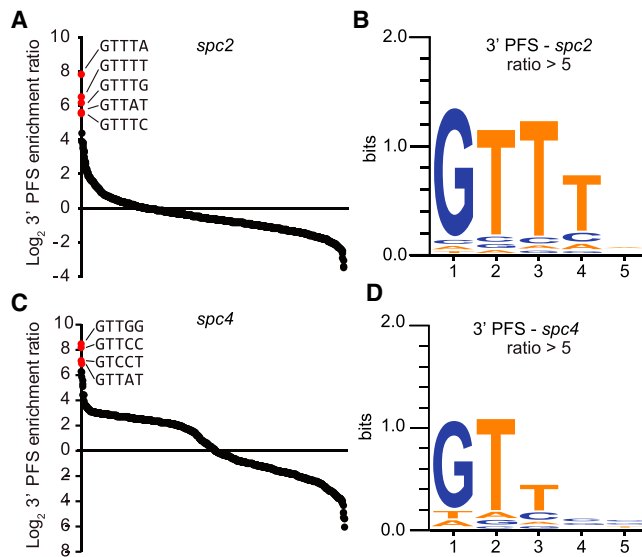


Figure 3. A GTT Sequence Immediately Downstream of the Target Protospacer Enables Escape from Type VI-A CRISPR Targeting
(A) Distribution of \log_2 enrichment ratios (WT/ Δ CRISPR) for all 1,024 3' flanking sequences for the *spc2* library. Top enriched sequences are indicated in red. (B) Weighted sequence logos for 3' target flanking sequences enriched more than 5-fold in the CRISPR+ strain for the *spc2* library. (C and D) Enrichment ratios (C) and sequence logo (D) for the *spc4* library. See also Figure S2.

3' and 5' PFS sequences was detected for both spacers. No particular sequences were specifically depleted in the wild-type strain at either side of the *spc2* (Figure S2B) or *spc4* (Figure S2C) target, suggesting that most sequences are efficiently targeted by the type VI-A CRISPR system and that a PAM is not required for targeting as in type I, II, and V systems. We then looked at sequences that were enriched in the wild-type strain. No consistently enriched sequences were detected in the 5' end of the spacer libraries for either target (Figure S2D). In contrast, we detected a group of related sequences on the 3' side of each protospacer that was enriched in the wild-type strain, suggesting that these targets escaped cleavage by Cas13. For the *spc2* target, the sequences began with GTTT (Figure 3A), a motif detected when all sequences that were over 5-fold enriched in wild-type were weighted for representation in the *spc2* library (Figure 3B). A similar sequence (GTT) was also enriched in the *spc4* library (Figures 3C and 3D). Interestingly, re-analysis of PFS data obtained via expressing *Leptotrichia shahii* Cas13 in *E. coli* (Abudayyeh et al., 2016) also showed the presence of a GTT motif (Figure S2E). In conclusion, our studies corroborate earlier findings indicating the absence of a PAM requirement for Cas13 targeting but also uncovered a previously unrecognized motif—GTT or GTTT—that, when present immediately downstream of the protospacer, prevents targeting.

Repeat-like Sequences Immediately Downstream of the Protospacer Enable Target Protection

Since the repeats of the *L. seeligeri* type VI-A CRISPR locus begin with the sequence 5'-GTTT-3', we investigated the effect

of the addition of repeat-like sequences downstream of the protospacer on immunity (Figure 4A). To do this, we used our conjugation assay to test immunity against the transfer of plasmids harboring 0 to 8 nt of repeat sequence downstream of the *spc2* protospacer (Figure 4B). All plasmids were transferred efficiently in the Δ CRISPR strain, and transformation of a target without homology to the CRISPR repeat in the 3' PFS was restricted and led to the formation of only a few very small transconjugant colonies. Addition of up to 3 nt of the repeat at the 3' end of the protospacer resulted in similar restriction. However, a 3' PFS with 4 repeat nucleotides conferred partial protection to the target plasmid, giving rise to more and intermediate-sized colonies. This result validated our previous target library findings, confirming that the enrichment for the 5'-GTTT-3' was a consequence of protection from type VI-A immunity. The addition of 5 repeat nucleotides improved protection, and 6 or more made the target plasmid completely resistant to type VI-A targeting, yielding many transconjugant colonies of wild-type size (Figure 4B). A similar protection was conferred by an 8-nt repeat downstream of the protospacer in pTarget(*spc4*), and, as expected from the result of the library experiment, replacement of the 5' PFS with 8 nt of repeat sequence did not affect type VI-A immunity against neither *spc2* nor *spc4* targets (Figure S3A). As a more sensitive assessment of growth rate of the different transconjugants, we examined their growth in liquid culture in the presence of target selection. As expected from the equivalent size of the Δ CRISPR transconjugant colonies on plates, their growth in liquid media was the same, regardless of the pTarget plasmid present (Figure 4C). Wild-type transconjugants, on the other hand, displayed different degrees of growth delays (Figure 4D) that were inversely correlated with the number of repeat-derived nucleotides at the 3' end of the protospacer in pTarget (except those with 7 and 8 repeat nucleotides, which grew indistinguishably). We also tested an analogous series of 3' PFS for the *spc4* target (Figure S3B). At least 6 nt were required for full protection from CRISPR-mediated restriction, although even 1 nt of repeat homology conferred some protective effect (Figures S3C and S3D).

To determine whether any individual nucleotide position is critical for protection, we mutated each of the 8 repeat nucleotides flanking *spc2* back to that present in the original 3' PFS (Figure 4E). First, we looked at pTarget conjugation (Figure 4F) and found that restoration of the original nucleotide at positions 8 to 4 (from the 3' end of the protospacer) was as protective as the full, 8-nt repeat sequence. However, restoration at positions 3 and 2 resulted in partial targeting (stronger in the presence of the position-2 mutation). Finally, restoration at position 1 resulted in wild-type levels of targeting. These results were corroborated after measuring the growth rates of the transconjugants. We found no differences in growth of the control Δ CRISPR transconjugants (Figure 4F), but for the wild-type transconjugants (Figure 4G), we observed normal growth for nucleotide restoration at positions 8 to 4, intermediate proliferation for positions 3 and 2 (worse growth for position 2), and the lowest growth rate for restoration of the first nucleotide (same growth as the full original sequence). These results showed that repeat nucleotides at positions 1, 2, and 3 are the most important for the protective effects of a repeat sequence placed downstream of the protospacer.

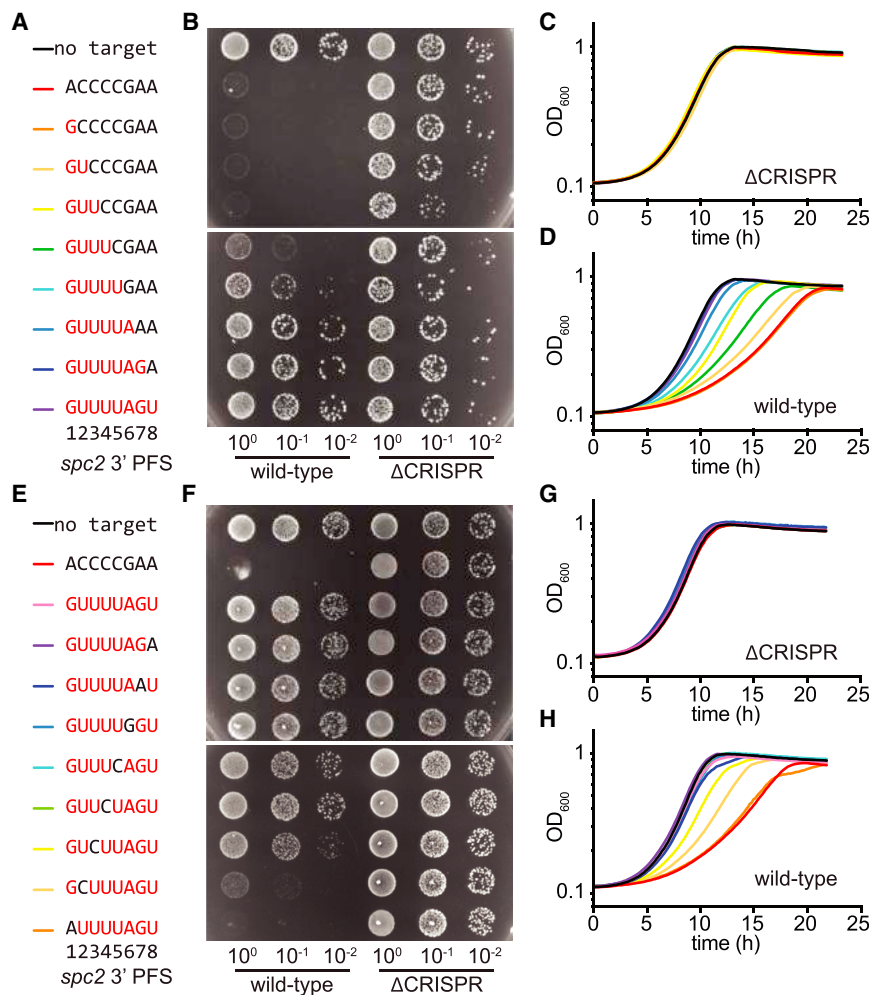


Figure 4. Repeat-like Sequences Immediately Downstream of the Protospacer Enable Target Protection

(A–D) Series of *spc2* pTarget plasmids containing repeat-derived sequences (indicated in red) (A) were tested for type VI CRISPR interference using a conjugation assay (B) and a liquid growth assay for Δ CRISPR (C) and wild-type (D).

(E–H) Series of *spc2* pTarget plasmids containing an 8-nt repeat sequence with a 1-nt mismatch at each position (E) tested via a conjugation assay (F) and a liquid growth assay for Δ CRISPR (G) and wild-type (H). Traces represent the mean from four biological replicates.

See also Figure S3.

expressing the wild-type crRNA, except for the target with a 6-nt repeat-derived 3' PFS (5'-GUUUUUA-3'), the transfer of all target plasmids harboring single-nucleotide mutations within this region was efficiently restricted (Figures 5B–5E). This result corroborates the data obtained for single-nucleotide mutations in Figure 4F in the context of a 6-nt repeat sequence downstream of the protospacer (different than the 8-nt repeat construct in our previous experiment) and expands the observation to all possible base changes in positions 1, 2, 3, and 4 of the repeat-derived 3' PFS. We then tested the transfer of each of these target plasmids into *Listeria* recipients expressing crRNAs with mutations in the corresponding positions of the tag region. When compared to the wild-type

Extended crRNA-Target Complementarity Prevents Type VI-A CRISPR Targeting

The protection afforded by the presence of a repeat sequence downstream of the protospacer could, in principle, be the result of (1) an extension of the complementarity between the crRNA and the target (5'-GUUUUAGU-3' in the target RNA; Figure 5A) or (2) a specific recognition of repeat-derived bases by the Cas13 nuclease that leads to an inhibition of target cleavage. To distinguish between these two possibilities, we tested whether mutations in the crRNA that disrupted complementarity could be rescued by compensatory mutations in the target 3' PFS. If specific bases of the 5'-GUUUUAGU-3' sequence were sensed by Cas13, the mutant targets would be protected from cleavage in spite of the restoration of complementarity by the compensatory mutation.

We constructed a set of target plasmids containing a 6-nt repeat sequence downstream of the protospacer in pTarget(*spc2*), with all possible bases at positions 1 to 4, where single-nucleotide deviations from the repeat sequence led to the restoration of targeting in our previous experiment (Figure 4F). None of these flanking sequences affected plasmid conjugation into Δ CRISPR *Listeria* cells (Figure S4). In *Listeria* recipients

crRNA, the mutation C > U in position 1 (Figure 5B) provided incomplete immunity against the transfer of wild-type pTarget(*spc2*) (with the non-repeat 3' PFS 5'-CAAA-3'), suggesting that the mutation partially affects crRNA processing and/or RNA cleavage by Cas13. The presence of a C or U in position 1 of the 3' PFS resulted in similarly incomplete targeting and, therefore, disrupted the protection conferred by the 6-nt repeat 3' PFS. However, the presence of a G or A in this position restored complete protection. These results are consistent with a role for complementarity-mediated protection, since the pairing U:G (a wobble base pair present in double-stranded RNA [dsRNA]; Varani and McClain, 2000) or U:A, but not the non-complementary U:C or U:U, prevented type VI-A immunity. The mutation A > U in position 2 of the crRNA tag (Figure 5C) did not affect Cas13 activity, since it provided full immunity against the transfer of wild-type pTarget(*spc2*). Similar targeting was observed with targets with mismatches (U:T and U:C) in this position, but protection was restored when base pairing was allowed (U:A and U:G). In the case of the A > C substitution in position 3 of the crRNA tag (Figure 5D), the mutation completely restricted the transfer of wild-type pTarget(*spc2*) but failed in the presence of the C:G compensatory mutation; the

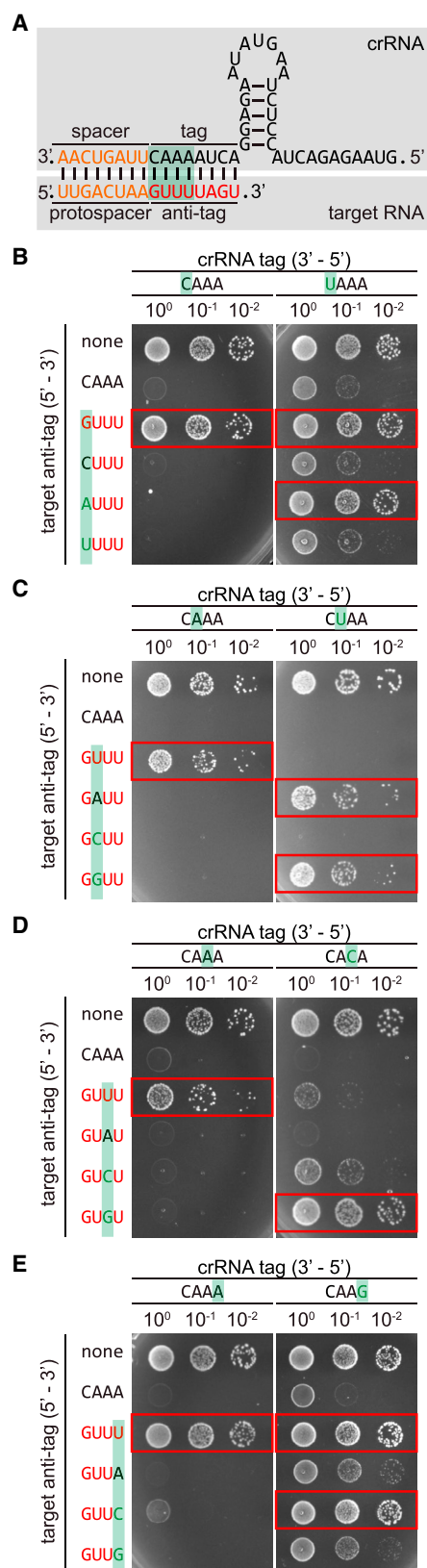


Figure 5. Extended crRNA-Target Complementarity Prevents Type VI-A CRISPR Targeting

(A) Schematic of type VI crRNA binding to RNA targets with crRNA tag complementarity. The spacer and protospacer are indicated in orange, the crRNA tag is indicated in black, and the complementary anti-tag is indicated in red. Nucleotides in the green boxed region were tested for participation in sensing tag:anti-tag complementarity.

(B–E) Conjugation assays were carried out with either wild-type *L. seeligeri* recipients or ones carrying mutations in the *spc2* crRNA tag at positions 1 (B), 2 (C), 3 (D), or 4 (E), with the mutated position highlighted in green. pTarget plasmids carried *spc2*-matching targets with an anti-tag sequence (indicated in red), except for mutations in the highlighted position. Combinations resulting in full tag:anti-tag complementarity (allowing G-U RNA wobble base pairing) are boxed in red.

See also Figure S4.

non-complementary targets at this position were either fully targeted (C:A) or partially targeted (C:U and C:C). Finally, the A > G mutation in position 4 (Figure 5E) provided incomplete immunity against the transfer of wild-type pTarget(*spc2*) when compared to the transfer of a target-less plasmid, suggesting a partial deficiency in Cas13 crRNA processing and/or targeting. Non-complementary targets in this position (G:A or G:G) were equally targeted, but the restoration of complementarity (G:U and G:C) completely disrupted type VI-A immunity against conjugation. Taken together, these results indicate that extended complementarity between the crRNA tag and the 3' PFS (hereinafter referred as the “anti-tag”) abrogates type VI-A CRISPR-Cas immunity in *L. seeligeri*.

Extended Complementarity Inhibits Cas13 *cis*- and *trans*-Cleavage *In Vitro*

To investigate the molecular details of the inhibitory effects of tag:anti-tag complementarity on Cas13 activity, we decided to test our findings using biochemical assays. Because we were unable to purify *L. seeligeri* Cas13, we used *Leptotrichia buccalis* Cas13 (LbuCas13). We expressed and purified the nuclease from *E. coli* and incubated it with a synthetic crRNA (harboring 21 nt of spacer sequence) and radiolabeled RNA targets as previously described (East-Seletsky et al., 2016; Liu et al., 2017a). We tested three different target sequences: a non-specific target, one containing a protospacer, and another in which the protospacer was followed by an 8-nt anti-tag (Figure 6A). We observed cleavage of the protospacer target but not of the non-specific target or anti-tag target (Figures 6B and S5A). We then tested the previously reported *trans*-RNA cleavage activity of LbuCas13 (East-Seletsky et al., 2016; Liu et al., 2017a) by radiolabeling the non-specific RNA and adding unlabeled target or anti-target-activating RNAs. We detected *trans*-RNA degradation only in the absence of the anti-tag sequence (Figure 6C). Altogether, these results demonstrate that the lack of type VI-A CRISPR-Cas immunity *in vivo* is due to the inactivation of Cas13 *cis*- and *trans*-RNase activity by the anti-tag target.

Next, we explored the mechanism behind the inhibition of Cas13 by the anti-tag target. Since *in vitro* assays only contain Cas13 and target and guide RNAs, the aforementioned results demonstrate that additional host factors are not required for Cas13 inhibition in the presence of the anti-tag. First we tested whether, as our *in vivo* data suggest, Cas13 inhibition requires the formation of an extended target RNA:crRNA duplex in the

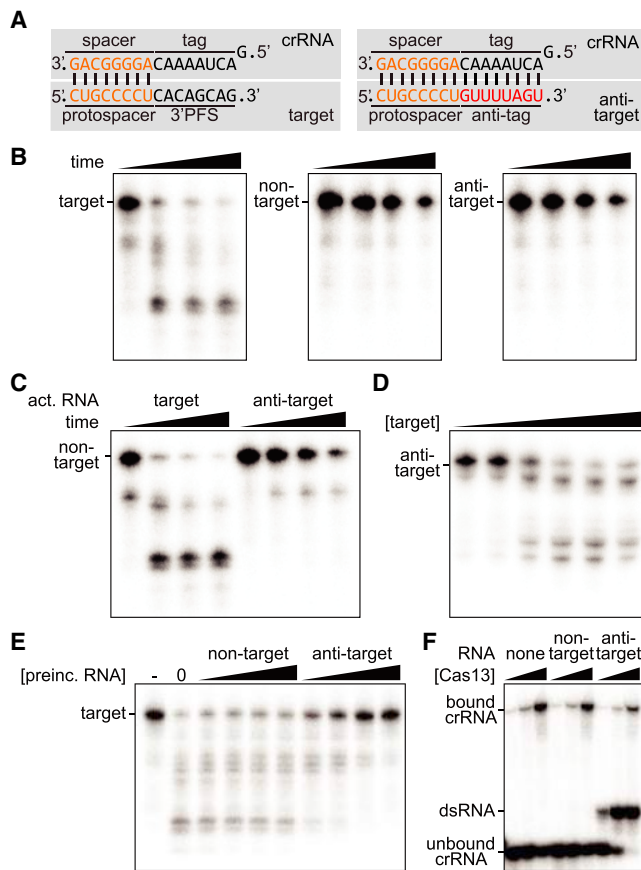


Figure 6. Extended Complementarity Inhibits Cas13 cis- and trans-Cleavage In Vitro

(A) A schematic showing protospacer-containing target RNA (left) with noncomplementary 3' extension and anti-target RNAs bearing an 8-nt anti-tag that extends the crRNA:target duplex.

(B) *In vitro* cis-RNA cleavage time course with 10 nM purified LbuCas13 and 10 nM labeled target, non-target, or anti-target RNA substrates. Reaction products were analyzed at 0, 5, 20, and 60 min of incubation.

(C) Cas13 *trans*-RNA cleavage assay. Labeled nontarget RNA substrates (10 nM) were incubated with 10 nM Cas13 ribonucleoprotein (RNP) and the indicated unlabeled activating RNA target (10 nM).

(D) *trans*-cleavage of 10 nM labeled anti-target by preincubation of 10 nM Cas13 with increasing amounts (0.01, 0.1, 1, 10, 100, and 1,000 nM) of activating target RNA.

(E) Inhibition of target cleavage by the addition of competing anti-target RNA. 10 nM target RNA was cleaved by Cas13 RNP in reactions pre-incubated with 10, 25, 50, or 100 nM nontarget or anti-target RNA.

(F) Electrophoretic mobility shift assay (EMSA) testing interaction between 1 nM crRNA and 0, 10, and 100 nM Cas13 in the presence of 100 nM competitor RNA.

See also Figure S5.

presence of the anti-tag. To address this, we tested whether anti-tag targets without access to the crRNA were substrates for activated Cas13, by initiating targeting reactions with LbuCas13 and an unlabeled target RNA and then adding a radiolabeled anti-tag target (Figure 6D). We observed cleavage of the anti-tag target under these conditions, indicating that inhibition of targeting mediated by the anti-tag only occurs when this

sequence is paired with the crRNA tag. Next, we determined whether tag:anti-tag interaction locks Cas13 in an inactive form incapable of cleaving a protospacer-only target. We pre-incubated the Cas13-crRNA complex with an unlabeled anti-tag protospacer or with unlabeled non-target RNA to control for the amount of total RNA in each reaction. Then, we added a radiolabeled target RNA to the reaction and looked for cleavage products. While preincubation with a non-specific RNA could not prevent the cleavage of the target RNA (the cleavage products were indistinguishable from the control without unlabeled RNA), preincubation with the anti-tag RNA inhibited target cleavage in a concentration-dependent manner (Figure 6E). To determine whether this inhibition, which was strongest at the higher concentrations of anti-tag RNA, was also possible at excess concentrations of the target RNA, we repeated the experiment with a constant concentration of non-specific or anti-tag RNA (100 nM) and tested the inhibition of Cas13a *trans*-RNase activity when activated using different concentrations of target RNA (up to 1,000 nM). We observed Cas13a inhibition even at the highest target RNA concentration (Figure S5B), a result that suggests that the anti-tag inhibitor locks Cas13a in an inactive form. Finally, to rule out the possibility that anti-tag inhibition is achieved through the sequestration of the crRNA guide away from Cas13a (i.e., during pre-incubation, the anti-tag RNA forms a dsRNA with the crRNA outside of the nuclease), we performed an electrophoretic mobility shift assay to assess whether the crRNA interaction with Cas13 was preserved after the addition of a large excess of anti-tag target RNA (anti-tag RNA:crRNA ratio of 100:1). Although we observed the formation of an anti-tag RNA:crRNA duplex, this was at the expense of the free crRNA (Figure 6F). Compared to the addition of a non-target RNA control, most of the Cas13a-bound crRNA remained bound in the presence of the anti-tag target, demonstrating that anti-tag inhibition does not work through the separation of the nuclease from its guide. Collectively, our *in vivo* and *in vitro* experiments demonstrate that RNA targets harboring an anti-tag sequence immediately downstream of the protospacer form a ribonucleoprotein complex that contains an extended dsRNA duplex with the tag sequence of the crRNA. This additional RNA complementarity locks the Cas13a complex into an inactive conformation unable to perform both *cis*- and *trans*-RNA degradation.

Anti-tag Inactivation of Cas13 Prevents Self-Targeting of Antisense CRISPR Transcripts

Our findings indicate that RNAs originating from antisense transcription of the CRISPR array will have a perfect anti-tag and should be spared from Cas13 cleavage. This would be similar to the mechanism used by type III systems to avoid self-targeting (Elmore et al., 2016; Kazlauskienė et al., 2016; Marraffini and Sontheimer, 2010). We checked for the presence of antisense CRISPR transcription in *L. seeligeri* by both northern blot and β -galactosidase transcriptional fusion assays (Figure S6). We did not detect antisense transcripts in either of these experiments, neither in the presence nor in the absence of a *spc4* target. Therefore, to test whether the pairing of tag with anti-tag could prevent self-targeting of the CRISPR array, we engineered plasmids with the CRISPR locus in the sense

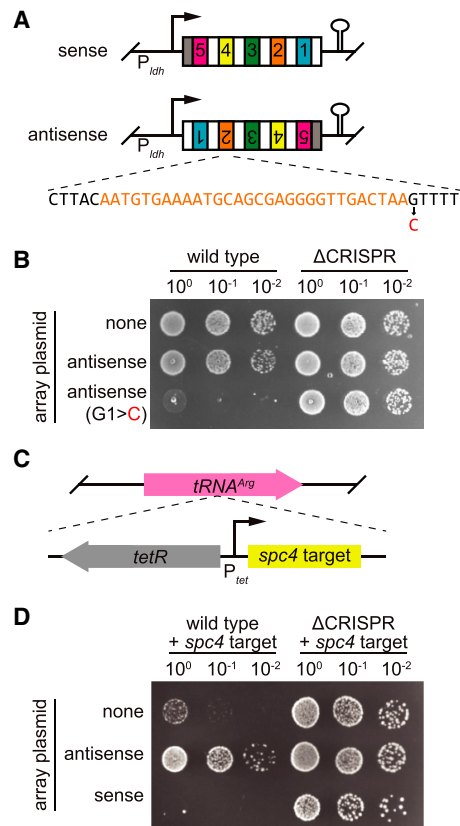


Figure 7. Anti-tag Inactivation of Cas13 Prevents Self-targeting of Antisense CRISPR Transcripts

(A) Plasmids engineered to constitutively express the CRISPR array in sense or antisense orientations. A variant of the antisense plasmid was constructed with a single mutation in the PFS flanking *spc2* (*spc* sequence is indicated in orange, repeat sequences are indicated in black, and mismatch is highlighted in red).

(B) Conjugation assay showing CRISPR-dependent toxicity of a single mismatch in an antisense CRISPR array transcript.

(C) An aTc-inducible target construct matching *spc4* was integrated into the *tRNA^{Arg}* locus of the *L. seeligeri* genome.

(D) Conjugation assay demonstrating inhibition of CRISPR interference by expression of antisense CRISPR array. Plasmids bearing a sense or antisense array were conjugated into wild-type (WT) or ΔCRISPR recipients carrying the inducible target and plated in the presence of 100 ng/mL aTc.

and antisense orientations with respect to the constitutive *ldh* promoter and followed by reverse-facing terminators to isolate the CRISPR sequences from transcription from other promoters (Figure 7A). As expected from our findings, the presence of an anti-tag sequence prevented the targeting of the perfectly matching protospacers within the antisense CRISPR transcript, which we confirmed was expressed (Figures 7B and S6B). In contrast, the introduction of a G > C mutation in position 1 of the anti-tag, which generates a mismatch with the crRNA tag, resulted in a strong type VI-A CRISPR-Cas response against the antisense CRISPR plasmid (Figure 7AB). These results exemplify the importance of the tag:anti-tag inhibition of Cas13 to prevent otherwise potentially toxic bidirectional transcription of the CRISPR array.

Given that (1) our *in vitro* findings showed that anti-tag targets prevent both *cis*- and *trans*-Cas13a RNase activities (Figure 6), and (2) antisense CRISPR transcripts contain anti-tags and are tolerated *in vivo*, we wondered whether antisense transcription of the CRISPR locus could inhibit the *trans*-RNA degradation by type VI-A systems. To test this, we integrated an anhydrotetracycline (aTc)-inducible, *spc4*-matching target into the *tRNA^{Arg}* gene of both wild-type and ΔCRISPR *L. seeligeri* strains (Figure 7C). The addition of aTc elicited a strong growth defect of wild-type, but not ΔCRISPR cells (Figure 7D). Therefore, we used this assay to determine whether antisense CRISPR transcripts could interfere with type VI-A immunity against the chromosomal target. We introduced the plasmids expressing the CRISPR locus in the sense and antisense orientations (Figure 7A) and added aTc. We found no immunity against the chromosomal target in the presence of the antisense CRISPR transcript (Figure 7D). These results show that antisense transcription of the CRISPR locus can inhibit Cas13a activity *in vivo*, and, therefore, it could be used for the regulation of the type VI-A CRISPR-Cas immune response.

DISCUSSION

Here, we have shown that type VI-A CRISPR-Cas immunity is inhibited by extended complementarity between the crRNA tag and the 3' protospacer flanking sequence (here named the "anti-tag"; Figure 5A). Our data indicate that this complementarity prevents targeting by *L. seeligeri* Cas13 *in vivo*, as well as by *L. buccalis* Cas13 *in vitro*. Biochemical assays indicate that anti-tag targets interfere with the activation of the Cas13:crRNA ribonucleoprotein complex through the direct annealing to the crRNA guide within the nuclease, preventing both *cis*- and *trans*-cleavage of RNA molecules. The presence of the same inhibitory mechanism in both LseCas13 and LbuCas13, which are only 20.8% identical, suggests that it is a widespread feature of type VI-A CRISPR-Cas systems. Given the recent repurposing of Cas13a as a tool for nucleic acid detection and RNA knock-down in eukaryotic cells (Abudayyeh et al., 2017; East-Seletsky et al., 2016; Gootenberg et al., 2017, 2018), our findings highlight important targeting rules for the design of effective crRNA guides in these technologies.

A previous screen reported that a single G in position 1 of the 3' PFS is sufficient to protect targets from cleavage by LshCas13a in an *E. coli* heterologous host (Abudayyeh et al., 2016). Our re-analysis of the LshCas13a 3' PFS screen data in *E. coli* indicated that highly protected targets contain extended repeat sequences in the 3' PFS, beyond the first G (Figure S2E). Therefore, we believe that both studies produced consistent screen results. However, during the validation of the screen data with individual targets, we found that 5–7 complementary nucleotides are required for full protection in the *L. seeligeri* natural host (Figures 6A–6D), whereas a single complementary G nucleotide is required in *E. coli* (Abudayyeh et al., 2016). We believe that this discrepancy could be due to (1) improper folding or activity of Cas13a in the heterologous host, resulting in the production of a weaker nuclease for which less tag:anti-tag pairing has a greater inhibitory effect, and/or (2) the use of different target sequences, whose nucleotide composition could

influence the effect of the 3' PFS on cleavage. Indeed, we found some spacer-specific differences when we compared the degrees of tag:anti-tag complementarity required to eliminate the immunity against *spc2* and *spc4* targets (Figures 4 and S3). These discrepancies highlight the importance of studying the biology of type VI systems in their natural hosts.

Whereas Cas13a cleaves upstream of the stem-loop structure formed by repeat sequences in the pre-crRNA of type VI-A systems, Cas13b cleaves downstream of this structure in type VI-B systems (Smargon et al., 2017). As a consequence of these cleavage differences, the crRNA tag sequence is located in the 5' end of type VI-A crRNAs and in the 3' of type VI-B crRNAs. The PFS requirements reported for type VI-B systems are also switched in orientation, and the presence of C on the 5' side of the protospacer prevents efficient targeting in heterologous hosts (Cox et al., 2017; Smargon et al., 2017). We speculate that, since the type VI-B repeats described so far begin with G, this nucleotide will be part of the crRNA tag, and therefore the presence of a 5' end anti-tag in type VI-B targets may inhibit Cas13b nuclease activity in the same way that a 3' end anti-tag inhibits Cas13a. Although for some Cas13 homologs no particular PFS requirements have been identified (Abudayyeh et al., 2017; Konermann et al., 2018; Yan et al., 2018), it remains to be determined whether the presence of an anti-tag flanking the protospacer prevents target cleavage. We suspect that the inhibition of Cas13a generated by the extension of complementarity between the crRNA and the target RNA could be a general feature of all type VI CRISPR-Cas systems. Understanding the effect of anti-tag sequences in other Cas13 homologs will be important for the investigation of the function of type VI systems both in their native bacteria and in heterologous eukaryotic hosts.

Tag:anti-tag inhibition of Cas13a targeting has parallels in type III CRISPR-Cas systems. In these systems, recognition of a complementary transcript by the crRNA guide within the Cas10-Csm (type III-A) or Cas10-Cmr (III-B) nuclease complex results in the specific cleavage of the target RNA and non-specific degradation of the transcribed DNA (Elmore et al., 2016; Estrella et al., 2016; Kazlauskienė et al., 2016; Samai et al., 2015). In contrast with the effect of the anti-tag in type VI-A CRISPR-Cas immunity, which prevents both specific and non-specific cleavage of RNA, tag:anti-tag pairing in type III systems does not affect cleavage of RNA by the Csm3/Cmr4 subunit but completely abolishes non-specific DNA degradation by the Cas10 nuclease (Kazlauskienė et al., 2016; Samai et al., 2015). Type III systems also express an RNase, Csm6 (III-A), or Csx1 (III-B), which, similarly to Cas13, contains a HEPN RNA degradation domain that hydrolyzes non-specific RNAs after recognition of an RNA target by the crRNA guide (Jiang et al., 2016; Niewoehner and Jinek, 2016). Csm6 and Csx1, however, are not part of the type III effector complexes, and, as opposed to Cas13, they do not carry a guide RNA themselves. Instead, the non-specific RNase activity is activated indirectly through the generation of a second messenger: upon crRNA recognition of the target RNA, the PALM domain of Cas10 converts ATP into a cyclic oligoadenylate product that allosterically activates Csm6 (Kazlauskienė et al., 2017; Niewoehner et al., 2017). It remains to be determined whether the interaction of tag and anti-tag in type III systems abolishes this activation.

What role might crRNA tag:anti-tag inhibition play during type VI-A CRISPR-Cas immunity? We can speculate about two possible scenarios where this inhibition will be beneficial to the host. First, similar to type III systems (Kazlauskienė et al., 2016; Marraffini and Sontheimer, 2010), we showed that type VI-A systems can use tag:anti-tag inhibition to prevent the triggering of Cas13a activity by antisense transcription of the CRISPR array (Figures 7A and 7B). Although we did not detect antisense CRISPR transcripts in *L. seeligeri*, such transcription could arise after the horizontal gene transfer of CRISPR systems (Godde and Bickerton, 2006). The random integration of a laterally transferred type VI-A CRISPR locus into the genome of the new host could result in toxic head-on transcription across the CRISPR array. If such scenarios were common, then type VI-A systems may benefit from a mechanism to avoid this form of auto-immunity. A second use of tag:anti-tag inhibition could be for the regulation of type VI-A immunity. Under circumstances where Cas13 activity is undesirable, controlled antisense CRISPR transcription could rapidly abrogate Cas13a activity, as we showed using an inducible promoter upstream of an inverted CRISPR array (Figures 7C and 7D). This mode of inactivation would be faster than the direct turnoff of crRNA or *cas13a* gene expression, since, in this case, the elimination of CRISPR activity will not be immediate but will depend on the turnover rate of the type VI-A ribonuclease complex. While it remains to be determined whether this type of regulation naturally occurs in microorganisms, tag:anti-tag inhibition of Cas13a activity could certainly be used to quickly turn off Cas13a-mediated knockdown of transcripts in eukaryotic cells.

STAR★METHODS

Detailed methods are provided in the online version of this paper and include the following:

- KEY RESOURCES TABLE
- CONTACT FOR REAGENT AND RESOURCE SHARING
- EXPERIMENTAL MODEL AND SUBJECT DETAILS
 - Bacterial strains and growth conditions
- METHOD DETAILS
 - Plasmid construction
 - *E. coli* – *L. seeligeri* conjugation
 - *L. seeligeri* strain construction
 - Northern blot analysis
 - RNA sequencing
 - PFS library construction and deep sequencing
 - Protein purification
 - *In vitro* RNA cleavage assays
 - Electrophoretic mobility shift assay
 - β -galactosidase assay
- QUANTIFICATION AND STATISTICAL ANALYSIS
- DATA AND SOFTWARE AVAILABILITY

SUPPLEMENTAL INFORMATION

Supplemental Information includes six figures and one data file and can be found with this article online at <https://doi.org/10.1016/j.molcel.2018.07.013>.

ACKNOWLEDGMENTS

We thank all members of the Marraffini lab for helpful discussion and encouragement, Daniel Portnoy for sharing *E. coli*-*Listeria* shuttle vectors pAM401-oriT and pPL2e, and Darren Higgins and Daniel Grubaugh for *Listeria* advice and sharing allelic exchange and conjugation protocols. A.J.M. was supported by a Merck fellowship and a Helen Hay Whitney postdoctoral fellowship. Support for this work comes from the NIH Director's Pioneer Award 1DP1GM128184-01 (to L.A.M.).

AUTHOR CONTRIBUTIONS

A.J.M. conducted the experiments. A.J.M. and L.A.M. designed the experiments and wrote the paper.

DECLARATION OF INTERESTS

The authors declare no competing interests.

Received: June 4, 2018

Revised: July 6, 2018

Accepted: July 12, 2018

Published: August 16, 2018

REFERENCES

- Abudayyeh, O.O., Gootenberg, J.S., Konermann, S., Joung, J., Slaymaker, I.M., Cox, D.B., Shmakov, S., Makarova, K.S., Semenova, E., Minakhin, L., et al. (2016). C2c2 is a single-component programmable RNA-guided RNA-targeting CRISPR effector. *Science* 353, aaf5573.
- Abudayyeh, O.O., Gootenberg, J.S., Essletzbichler, P., Han, S., Joung, J., Belanto, J.J., Verdine, V., Cox, D.B.T., Kellner, M.J., Regev, A., et al. (2017). RNA targeting with CRISPR-Cas13. *Nature* 550, 280–284.
- Barrangou, R., Fremaux, C., Deveau, H., Richards, M., Boyaval, P., Moineau, S., Romero, D.A., and Horvath, P. (2007). CRISPR provides acquired resistance against viruses in prokaryotes. *Science* 315, 1709–1712.
- Brouns, S.J., Jore, M.M., Lundgren, M., Westra, E.R., Slijkhuys, R.J., Snijders, A.P., Dickman, M.J., Makarova, K.S., Koonin, E.V., and van der Oost, J. (2008). Small CRISPR RNAs guide antiviral defense in prokaryotes. *Science* 321, 960–964.
- Carver, T., Harris, S.R., Berriman, M., Parkhill, J., and McQuillan, J.A. (2012). Artemis: an integrated platform for visualization and analysis of high-throughput sequence-based experimental data. *Bioinformatics* 28, 464–469.
- Cox, D.B.T., Gootenberg, J.S., Abudayyeh, O.O., Franklin, B., Kellner, M.J., Joung, J., and Zhang, F. (2017). RNA editing with CRISPR-Cas13. *Science* 358, 1019–1027.
- Deltcheva, E., Chylinski, K., Sharma, C.M., Gonzales, K., Chao, Y., Pirzada, Z.A., Eckert, M.R., Vogel, J., and Charpentier, E. (2011). CRISPR RNA maturation by trans-encoded small RNA and host factor RNase III. *Nature* 471, 602–607.
- Deveau, H., Barrangou, R., Garneau, J.E., Labonté, J., Fremaux, C., Boyaval, P., Romero, D.A., Horvath, P., and Moineau, S. (2008). Phage response to CRISPR-encoded resistance in *Streptococcus thermophilus*. *J. Bacteriol.* 190, 1390–1400.
- Dobin, A., Davis, C.A., Schlesinger, F., Drenkow, J., Zaleski, C., Jha, S., Batut, P., Chaisson, M., and Gingeras, T.R. (2013). STAR: ultrafast universal RNA-seq aligner. *Bioinformatics* 29, 15–21.
- East-Seletsky, A., O'Connell, M.R., Knight, S.C., Burstein, D., Cate, J.H., Tjian, R., and Doudna, J.A. (2016). Two distinct RNase activities of CRISPR-C2c2 enable guide-RNA processing and RNA detection. *Nature* 538, 270–273.
- Elmore, J.R., Sheppard, N.F., Ramia, N., Deighan, T., Li, H., Terns, R.M., and Terns, M.P. (2016). Bipartite recognition of target RNAs activates DNA cleavage by the type III-B CRISPR-Cas system. *Genes Dev.* 30, 447–459.
- Estrella, M.A., Kuo, F.T., and Bailey, S. (2016). RNA-activated DNA cleavage by the type III-B CRISPR-Cas effector complex. *Genes Dev.* 30, 460–470.
- Gasiunas, G., Barrangou, R., Horvath, P., and Siksnys, V. (2012). Cas9-crRNA ribonucleoprotein complex mediates specific DNA cleavage for adaptive immunity in bacteria. *Proc. Natl. Acad. Sci. USA* 109, E2579–E2586.
- Godde, J.S., and Bickerton, A. (2006). The repetitive DNA elements called CRISPRs and their associated genes: evidence of horizontal transfer among prokaryotes. *J. Mol. Evol.* 62, 718–729.
- Gootenberg, J.S., Abudayyeh, O.O., Lee, J.W., Essletzbichler, P., Dy, A.J., Joung, J., Verdine, V., Donghia, N., Daringer, N.M., Freije, C.A., et al. (2017). Nucleic acid detection with CRISPR-Cas13a/C2c2. *Science* 356, 438–442.
- Gootenberg, J.S., Abudayyeh, O.O., Kellner, M.J., Joung, J., Collins, J.J., and Zhang, F. (2018). Multiplexed and portable nucleic acid detection platform with Cas13, Cas12a, and Csm6. *Science* 360, 439–444.
- Hale, C., Kleppe, K., Terns, R.M., and Terns, M.P. (2008). Prokaryotic silencing (psi)RNAs in *Pyrococcus furiosus*. *RNA* 14, 2572–2579.
- Jiang, W., Samai, P., and Marraffini, L.A. (2016). Degradation of phage transcripts by CRISPR-associated RNases enables type III CRISPR-Cas immunity. *Cell* 164, 710–721.
- Jinek, M., Chylinski, K., Fonfara, I., Hauer, M., Doudna, J.A., and Charpentier, E. (2012). A programmable dual-RNA-guided DNA endonuclease in adaptive bacterial immunity. *Science* 337, 816–821.
- Kazlauskienė, M., Tamulaitis, G., Kostiuik, G., Venclovas, Č., and Siksnys, V. (2016). Spatiotemporal control of type III-A CRISPR-Cas immunity: coupling DNA degradation with the target RNA recognition. *Mol. Cell* 62, 295–306.
- Kazlauskienė, M., Kostiuik, G., Venclovas, Č., Tamulaitis, G., and Siksnys, V. (2017). A cyclic oligonucleotide signaling pathway in type III CRISPR-Cas systems. *Science* 357, 605–609.
- Konermann, S., Lott, P., Brideau, N.J., Oki, J., Shokhiev, M.N., and Hsu, P.D. (2018). Transcriptome engineering with RNA-targeting type VI-D CRISPR effectors. *Cell* 173, 665–676.e14.
- Lauer, P., Chow, M.Y., Loessner, M.J., Portnoy, D.A., and Calendar, R. (2002). Construction, characterization, and use of two *Listeria monocytogenes* site-specific phage integration vectors. *J. Bacteriol.* 184, 4177–4186.
- Lillestøl, R.K., Shah, S.A., Brügger, K., Redder, P., Phan, H., Christiansen, J., and Garrett, R.A. (2009). CRISPR families of the crenarchaeal genus *Sulfolobus*: bidirectional transcription and dynamic properties. *Mol. Microbiol.* 72, 259–272.
- Liu, L., Li, X., Ma, J., Li, Z., You, L., Wang, J., Wang, M., Zhang, X., and Wang, Y. (2017a). The molecular architecture for RNA-guided RNA cleavage by Cas13a. *Cell* 170, 714–726.e10.
- Liu, L., Li, X., Wang, J., Wang, M., Chen, P., Yin, M., Li, J., Sheng, G., and Wang, Y. (2017b). Two distant catalytic sites are responsible for C2c2 RNase activities. *Cell* 168, 121–134.e12.
- Makarova, K.S., Wolf, Y.I., Alkhnbashi, O.S., Costa, F., Shah, S.A., Saunders, S.J., Barrangou, R., Brouns, S.J., Charpentier, E., Haft, D.H., et al. (2015). An updated evolutionary classification of CRISPR-Cas systems. *Nat. Rev. Microbiol.* 13, 722–736.
- Marraffini, L.A., and Sontheimer, E.J. (2008). CRISPR interference limits horizontal gene transfer in staphylococci by targeting DNA. *Science* 322, 1843–1845.
- Marraffini, L.A., and Sontheimer, E.J. (2010). Self versus non-self discrimination during CRISPR RNA-directed immunity. *Nature* 463, 568–571.
- Myhrvold, C., Freije, C.A., Gootenberg, J.S., Abudayyeh, O.O., Metsky, H.C., Durbin, A.F., Kellner, M.J., Tan, A.L., Paul, L.M., Parham, L.A., et al. (2018). Field-deployable viral diagnostics using CRISPR-Cas13. *Science* 360, 444–448.
- Niewoehner, O., and Jinek, M. (2016). Structural basis for the endonuclease activity of the type III-A CRISPR-associated protein Csm6. *RNA* 22, 318–329.
- Niewoehner, O., Garcia-Doval, C., Rostøl, J.T., Berk, C., Schwede, F., Bigler, L., Hall, J., Marraffini, L.A., and Jinek, M. (2017). Type III CRISPR-Cas systems produce cyclic oligoadenylate second messengers. *Nature* 548, 543–548.

- Pyenson, N.C., Gayvert, K., Varble, A., Elemento, O., and Marraffini, L.A. (2017). Broad targeting specificity during bacterial type III CRISPR-Cas immunity constrains viral escape. *Cell Host Microbe* 22, 343–353.e43.
- Samai, P., Pyenson, N., Jiang, W., Goldberg, G.W., Hatoum-Aslan, A., and Marraffini, L.A. (2015). Co-transcriptional DNA and RNA cleavage during type III CRISPR-Cas immunity. *Cell* 161, 1164–1174.
- Sauer, J.D., Witte, C.E., Zemansky, J., Hanson, B., Lauer, P., and Portnoy, D.A. (2010). *Listeria monocytogenes* triggers AIM2-mediated pyroptosis upon infrequent bacteriolysis in the macrophage cytosol. *Cell Host Microbe* 7, 412–419.
- Semenova, E., Jore, M.M., Datsenko, K.A., Semenova, A., Westra, E.R., Wanner, B., van der Oost, J., Brouns, S.J., and Severinov, K. (2011). Interference by clustered regularly interspaced short palindromic repeat (CRISPR) RNA is governed by a seed sequence. *Proc. Natl. Acad. Sci. USA* 108, 10098–10103.
- Shmakov, S., Smargon, A., Scott, D., Cox, D., Pyzocha, N., Yan, W., Abudayyeh, O.O., Gootenberg, J.S., Makarova, K.S., Wolf, Y.I., et al. (2017). Diversity and evolution of class 2 CRISPR-Cas systems. *Nat. Rev. Microbiol.* 15, 169–182.
- Smargon, A.A., Cox, D.B., Pyzocha, N.K., Zheng, K., Slaymaker, I.M., Gootenberg, J.S., Abudayyeh, O.A., Essletzbichler, P., Shmakov, S., Makarova, K.S., et al. (2017). Cas13b Is a Type VI-B CRISPR-Associated RNA-Guided RNase Differentially Regulated by Accessory Proteins Csx27 and Csx28. *Mol. Cell* 65, 618–630.e17.
- Varani, G., and McClain, W.H. (2000). The G x U wobble base pair. A fundamental building block of RNA structure crucial to RNA function in diverse biological systems. *EMBO Rep.* 1, 18–23.
- Yan, W.X., Chong, S., Zhang, H., Makarova, K.S., Koonin, E.V., Cheng, D.R., and Scott, D.A. (2018). Cas13d is a compact RNA-targeting type VI CRISPR effector positively modulated by a WYL-domain-containing accessory protein. *Mol. Cell* 70, 327–339.e25.
- Zetsche, B., Gootenberg, J.S., Abudayyeh, O.O., Slaymaker, I.M., Makarova, K.S., Essletzbichler, P., Volz, S.E., Joung, J., van der Oost, J., Regev, A., et al. (2015). Cpf1 is a single RNA-guided endonuclease of a class 2 CRISPR-Cas system. *Cell* 163, 759–771.

STAR★METHODS

KEY RESOURCES TABLE

REAGENT or RESOURCE	SOURCE	IDENTIFIER
Bacterial and Virus Strains		
<i>Listeria seeligeri</i> Rocourt and Grimont	ATCC	35967
<i>Listeria seeligeri</i> ΔCRISPR	This paper	N/A
<i>Escherichia coli</i> SM10	Darren Higgins, Harvard Medical School	N/A
Deposited Data		
PFS screen and RNA sequencing of <i>L. seeligeri</i> samples	This paper	SRA: SRP142551
PFS screen from <i>Leptotrichia shahii</i> type VI locus in <i>E. coli</i>	Abudayyeh et al., 2016	SRA: SRX1820082, SRX1820086
Oligonucleotides		
See Data S1	This paper	N/A
Recombinant DNA		
See Data S1	This paper	N/A

CONTACT FOR REAGENT AND RESOURCE SHARING

Further information and requests for resources and reagents should be directed to and will be fulfilled by the Lead Contact, Luciano Marraffini (marraffini@rockefeller.edu).

EXPERIMENTAL MODEL AND SUBJECT DETAILS

Bacterial strains and growth conditions

All *L. seeligeri* strains were derived from ATCC strain 35967 (Rocourt and Grimont), and were propagated in Brain Heart Infusion (BHI) broth or agar at 30°C. Constructs were cloned in *E. coli* DH5α, miniprep, and transformed into the conjugative donor strain *E. coli* SM10 for conjugative mating. All *E. coli* strains were cultured in Lysogeny Broth (LB) at 37°C.

METHOD DETAILS

Plasmid construction

The broad host range conjugative vector pAM401-oriT ([Sauer et al., 2010](#)) was used to construct pAM8 by replacement of its gram-negative chloramphenicol resistance cassette by the ampicillin resistant cassette of pUC19. pTarget plasmids were constructed by the addition of a protospacer downstream of the Gram-positive chloramphenicol resistance gene of pAM8. To construct pCRISPR plasmids, the *L. seeligeri* CRISPR locus was inserted into the PSA site-specific integrating vector pPL2e ([Lauer et al., 2002](#)). Lists of strains, plasmids, and oligonucleotide primers, along with details of plasmid construction can be found in [Data S1](#).

E. coli – *L. seeligeri* conjugation

Donor *E. coli* SM10 strains carrying *E. coli*-*Listeria* shuttle vectors were cultured in LB containing 100 μg/mL ampicillin (for pAM8-derived vectors) or 25 μg/mL chloramphenicol (for pPL2e-derived vectors). Recipient *L. seeligeri* strains were cultured in BHI. 100 μL each of donor and recipient culture were combined in 10 mL BHI, and concentrated onto a 0.45 μm membrane filter, which was then overlaid onto a BHI agar plate containing 8 μg/ml oxacillin, which weakens the cell wall, enhancing conjugation. Mating plates were incubated for 4 hr at 37°C, then cells were resuspended in 2 mL BHI, diluted as indicated, and plated at 30°C on selective media containing 50 μg/mL nalidixic acid (selects against donor). Selection for plasmid recipients was done with either 15 μg/mL chloramphenicol (for pAM8-derived vectors) or 1 μg/mL erythromycin (for pPL2e-derived vectors). Plates were incubated for 72 hr before imaging.

L. seeligeri strain construction

Allelic replacement in *L. seeligeri* was conducted using a “loop in, loop out” strategy, illustrated in [Figure S1](#). 1 kb homologous sequences flanking each side of the region to be replaced were cloned into a suicide plasmid unable to replicate in *L. seeligeri*.

The plasmid carries a gram negative origin of replication, an oriT sequence for conjugative transfer, a *lacZ* gene (*G. stearothermophilus bgaB*), and a gram positive chloramphenicol resistance marker. This plasmid was transferred to *L. seeligeri* via conjugation as described above, and 100 μ L of resuspended cells was plated for selection on 50 μ g/mL nalidixic acid and 15 μ g/mL chloramphenicol. Isolated transconjugants (integrants) were streak-purified and confirmed *lacZ*⁺ by patching on BHI plates containing 100 μ g/mL 5-Bromo-4-Chloro-3-Indolyl β -D-Galactopyranoside (X-gal). Integrants were passaged (grown to saturation, then diluted 1000 fold) four times in BHI without selection. Passaged cultures were diluted and plated on BHI X-gal, and incubated 2-3 days at 37°C. White (*lacZ*⁻) colonies (excisants) were isolated, cultured in BHI, and chromosomal DNA was prepared by lysozyme treatment followed by phenol-chloroform extraction. Each excisant was checked for the deletion by PCR using primers flanking the desired deletion, and Sanger-sequenced.

Northern blot analysis

RNA was isolated from 1 mL of *L. seeligeri* culture at OD₆₀₀ 0.5. Cell pellets were resuspended in 80 μ L RNase-free PBS, and lysed by a 5 min treatment with lysozyme at 20 μ g/mL, followed by the addition of 1% sarkosyl. RNA was purified from these lysates using the Zymo Research Direct-zol RNA MiniPrep Plus kit according to the manufacturer's instructions. For Northern blot analysis, 20 μ g RNA per sample was diluted in RNA loading dye and separated by gel electrophoresis on a 6% denaturing TBE-urea polyacrylamide gel. RNA was transferred to an Invitrogen BrightStar Plus nylon membrane using a semi-dry transfer apparatus. RNA was fixed to membranes using a Stratalinker UV crosslinker (Optimal Crosslinking setting). Membranes were pre-hybridized 30 min at 42°C in 2X SSC 1% SDS + 0.1 mg/mL denatured salmon sperm DNA. 250 pmol ssDNA probe was labeled with 20 μ Ci γ -³²P-ATP, purified using an Illustra MicroSpin G-50 column, and hybridized to the membrane overnight at 42°C. Membranes were washed twice with 2X SSC 0.1% SDS, once with 1X SSC 0.1% SDS, then exposed to a phosphoscreen for 24 hr, and imaged using a Beckman Coulter FLA7000IP Typhoon storage phosphorimager.

RNA sequencing

L. seeligeri RNA samples isolated as described above were prepared for RNA sequencing by depletion of ribosomal RNA using the Ribo-Zero rRNA removal (Gram Positive Bacteria) kit (Illumina) according to the manufacturer's instructions. The remaining RNA was prepared for deep sequencing with the TruSeq Stranded mRNA Library Prep kit (Illumina), and sequenced on the MiSeq platform using a 150 cycle cartridge (v3 reagents) on a single-end run. Reads were quality-trimmed and mapped to the pAM8 plasmid sequence using STAR (Dobin et al., 2013), and coverage was visualized with Artemis (Carver et al., 2012). Raw sequencing reads have been deposited to SRA: SRP142551.

PFS library construction and deep sequencing

Templates for library construction were amplified from pAM8 using oAM288+oAM185 (first fragment) and oAM288+oAM183 (second fragment). A second round of amplification introduced the protospacer and five adjacent randomized nucleotides. PFS libraries were constructed by amplification of the first round product with oAM290+oAM185 (spc2, 3' PFS), oAM291+oAM183 (spc2, 5' PFS), oAM292+oAM185 (spc4, 3' PFS), or oAM293+oAM183 (spc4, 5' PFS). These products were ligated to the appropriate acceptor (amplified with oAM246+oAM183 (spc2, 3' PFS), oAM245+oAM185 (spc2, 5' PFS), oAM250+oAM183 (spc4, 3' PFS), or oAM249+oAM185 (spc4, 5' PFS) via Gibson assembly to circularize the plasmid. Gibson products were transformed into NEB5 α competent cells selecting on ampicillin and 20,000 transformants were isolated for each library. Transformants were pooled, plasmids were isolated and transformed into *E. coli* SM10 (selecting on ampicillin) for conjugation. Transformants were pooled and inoculated into LB amp for mating. 100 μ L donor and recipient cultures were mated as described above, and transconjugants were selected on BHI agar containing nalidixic acid and chloramphenicol at 30°C. 20,000 transconjugants were selected and pooled. Target plasmids were isolated by resuspending pooled cell pellets in 250 μ L QIAGEN Miniprep buffer P1, adding 1mg lysozyme, incubating 37°C 10 min and proceeding with the miniprep protocol according to the manufacturer's instructions. Target amplicon was amplified with oAM334 and oAM336 using 10 ng plasmid as template. PCR products were prepared for sequencing using the TruSeq Nano DNA LT kit and sequencing was carried out with an Illumina MiSeq system using a 150 cycle cartridge (v3 reagents) on a single-end run. Target sequences were extracted and PFS sequences tabulated and sorted using standard UNIX commands. Raw sequence reads have been uploaded to SRA: SRP142551. Normalized PFS counts for each target and strain are available in [Data S1](#).

Protein purification

His6-MBP-LbuCas13 was purified essentially as previously described. Briefly, the *E. coli* BL21 (DE3) Rosetta2 strain were transformed with the LbuCas13 expression plasmid (Addgene), and fresh transformants were grown to OD₆₀₀ = 0.4 in LB + ampicillin, then diluted in 1L 2xYT broth + ampicillin and grown at 37°C to OD₆₀₀ = 0.6. Then, IPTG was added to 1mM and expression was carried out overnight at 16°C. Cells were pelleted and lysed by lysozyme treatment and sonication in lysis buffer (50mM Tris pH 7.0, 0.5M NaCl, 5% glycerol, 1mM DTT). Clarified lysates were applied to pre-equilibrated amylose resin (NEB), washed with 25 column volumes of lysis buffer, and eluted with the same buffer containing 10mM maltose. Eluate was cleaved with TEV protease at a 100:1 molar ratio overnight at 4°C, and untagged LbuCas13 was isolated from cleaved tag by gel filtration chromatography (isocratic elution). A single disperse peak contained purified untagged LbuCas13. Fractions were concentrated to 1 μ M and flash-frozen.

In vitro RNA cleavage assays

crRNA and ssRNA targets were commercially synthesized (IDT, sequences available in [Data S1](#)), labeled at 1 μ M with T4 polynucleotide kinase and 10 μ Ci γ -³²P-ATP, and purified using Illustra MicroSpin G-50 columns. Cleavage reactions were carried out in 10 mM HEPES pH 7.0, 50 mM KCl, 5 mM MgCl₂, and 5% glycerol. LbuCas13, crRNA and labeled targets were combined, each at 10 nM, and reactions were performed at room temperature for 20–60 min (as indicated). An equal volume of 2X formamide RNA sample buffer was added to each reaction, samples were boiled 5 min, cooled on ice 2 min, and cleavage products were resolved on 15% TBE-urea denaturing PAGE gels. Gels were exposed to a phosphoscreen for 1 hr and imaged using a Beckman Coulter FLA7000IP Typhoon storage phosphorimager.

Electrophoretic mobility shift assay

Commercially synthesized crRNA was 5' end-labeled as described above. 1 nM labeled crRNA was combined with 0, 10, or 100 nM LbuCas13 and when indicated, 100 nM unlabeled competitor RNA. Binding reactions were performed for 90 min at room temperature in 20 mM HEPES pH 7.0, 50 mM KCl, 10 μ g/mL bovine serum albumin, 100 μ g/mL salmon sperm DNA, 0.01% Triton X-100, and 5% glycerol. Samples were resuspended in native PAGE sample buffer, and resolved by 8% nondenaturing TBE PAGE at 4°C. Gels were exposed to a phosphoscreen for 1 hr and imaged using a Beckman Coulter FLA7000IP Typhoon storage phosphorimager.

β -galactosidase assay

Gene expression experiments were performed using 1 mL samples of exponentially growing cultures resuspended in 1 mL Z buffer (100 mM phosphate buffer pH 7.4, 10 mM KCl, 1 mM MgSO₄, 50 mM β -mercaptoethanol, 1 mg/mL lysozyme). Samples were incubated at 37°C 5 min before adding 200 μ L 4 mg/mL o-nitrophenyl- β -D-galactopyranoside (ONPG) and then transferred to 55°C for measurements of heat-stable β -galactosidase activity. Reactions were quenched with 500 μ L 1M Na₂CO₃, insoluble debris pelleted, and absorbance measurements were taken at 420 nm and 550 nm.

QUANTIFICATION AND STATISTICAL ANALYSIS

For quantification of deep sequencing reads in the *L. seeligeri* PFS screen, flanking sequences were counted in the wild-type and Δ CRISPR libraries, and normalized to the total number of reads for each library. For each of the 1024 flanking sequences, the WT: Δ CRISPR normalized abundance ratio was calculated and plotted. For growth curves in [Figure 2](#), error bars represent standard error of the mean from four biological replicates. For β -galactosidase assays in [Figure S6](#), error bars represent standard error of the mean from two biological replicates.

DATA AND SOFTWARE AVAILABILITY

The accession number for the raw PFS screen data related to [Figure 3](#) and raw RNA-seq reads related to [Figure S1](#) is SRA: SRP142551.

Molecular Cell, Volume 71

Supplemental Information

**RNA Guide Complementarity Prevents
Self-Targeting in Type VI CRISPR Systems**

Alexander J. Meeske and Luciano A. Marraffini

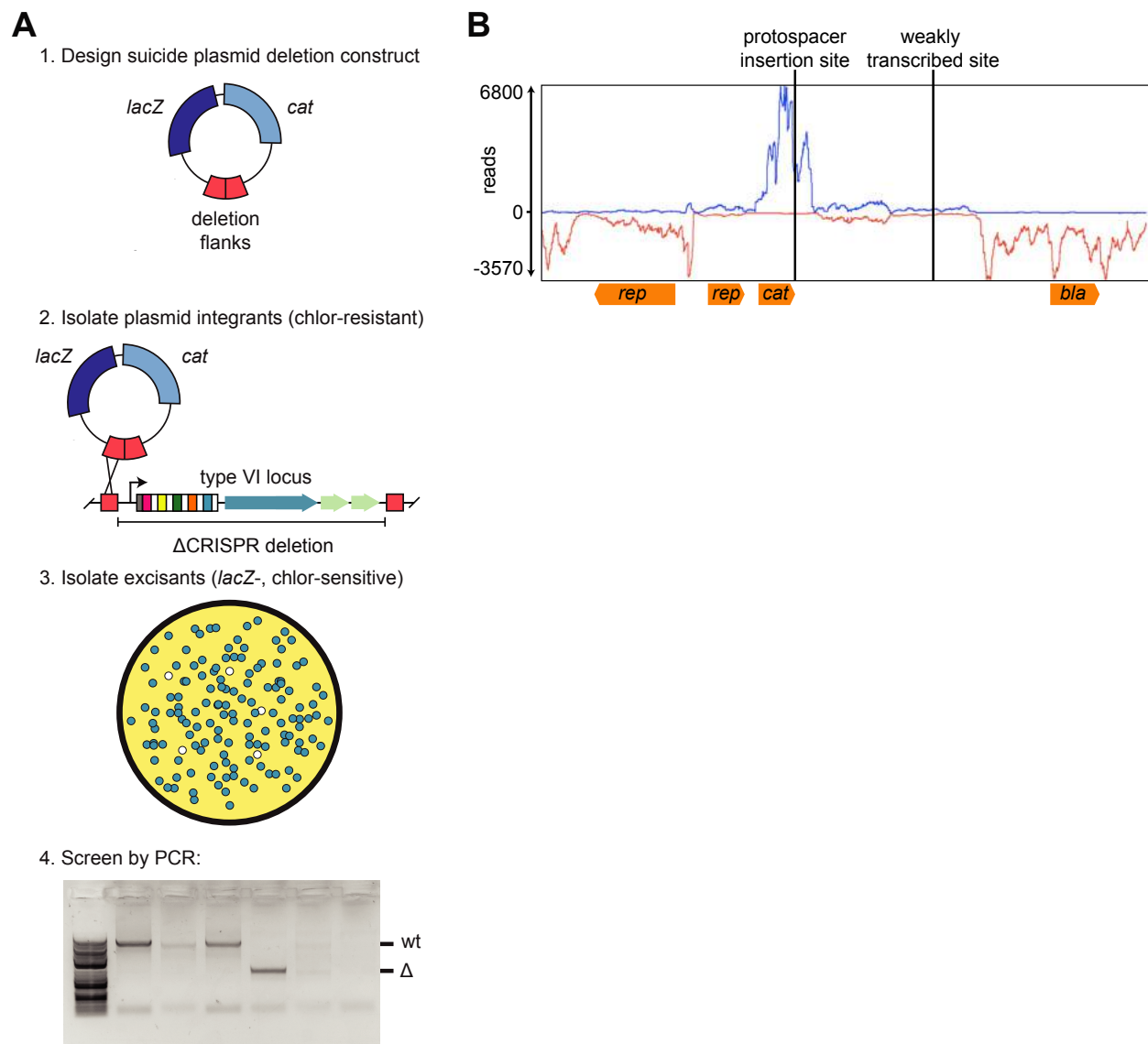


Figure S1: *Listeria seeligeri* strain construction and pTarget plasmids, related to Fig. 1. **A.** Four step protocol for generating knockouts and knockins in *Listeria seeligeri*. 1. The mutant allele is cloned into a suicide vector encoding a chloramphenicol resistance cassette for selection in *L. seeligeri*, as well as a *lacZ* gene as a plasmid reporter (generates blue color on X-gal plates). Once cloned, the allelic exchange construct is transformed into an SM10 *E. coli* strain for conjugative mating into *L. seeligeri*. 2. The suicide plasmid is introduced into *L. seeligeri* via conjugative mating, selecting on media containing chloramphenicol (15 $\mu\text{g/mL}$) and nalidixic acid (50 $\mu\text{g/mL}$) to select for plasmid integration and eliminate *E. coli* donor, respectively. Integrants are isolated by streaking on the same media. 3. Isolates are passaged twice in liquid culture without selection to allow the plasmid to be excised. Cultures are diluted and plated onto media containing X-gal, and after two days blue colonies are apparent. White colonies (excisants) are restreaked and confirmed to be chloramphenicol sensitive. 4. Excisants are screened by PCR and Sanger sequencing to check for the mutant allele. **B.** Stranded RNAseq coverage plot of *L. seeligeri* pTarget plasmid, showing protospacer insertion sites in 3' UTR of *cat* gene and weakly transcribed downstream site. Reads from top strand are in blue, bottom strand in red.

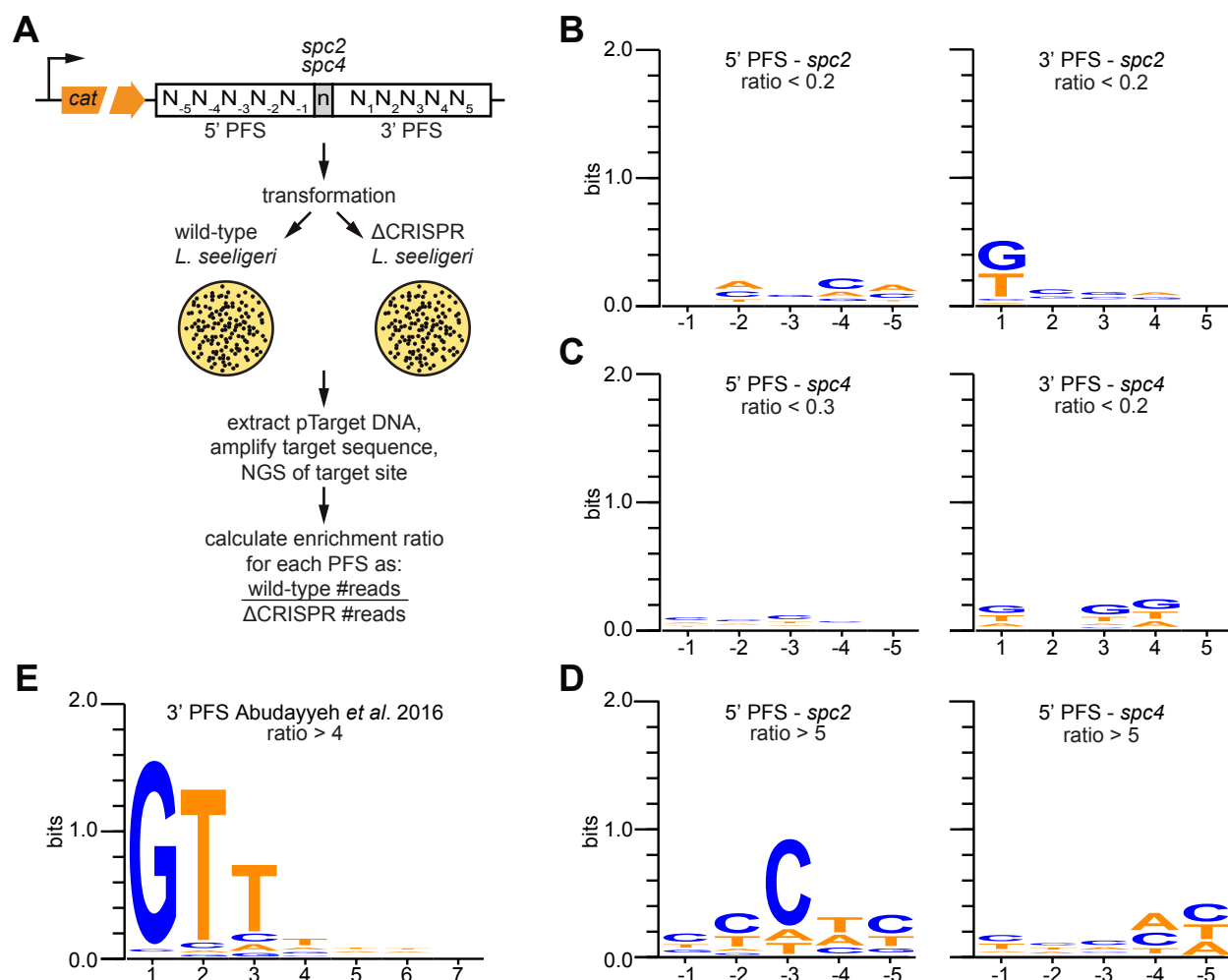


Figure S2: PFS screening strategy, targeted and enriched flanking sequences, related to Fig. 3.

A. Screening strategy to identify protospacer flanking sequence (PFS) requirements of the *L. seeligeri* type VI CRISPR system. Five randomized nucleotides were introduced at the 5' or 3' end of the *spc2* or *spc4* target sequence and these libraries were transformed into wild-type and Δ CRISPR *L. seeligeri* by conjugation. Transconjugants were pooled, target plasmids were isolated and the target flanking sites were deep sequenced. Flanking sequence representation was normalized to total reads and the WT: Δ CRISPR ratio was calculated for each 5nt sequence. **B.** Weighted sequence logos for 3' target flanking sequences depleted more than five fold in the wild type strain. Logos representing the 5' and 3' PFS from the *spc2* (**B**) and *spc4* (**C**) libraries are both shown. **D.** Weighted sequence logos for 5' target flanking sequences enriched more than five-fold in the CRISPR+ strain for each library. **E.** Sequence logos for 3' target flanking sequences enriched more than four-fold in the LshCas13 beta lactamase PFS screen from Abudayyeh *et al.* 2016.

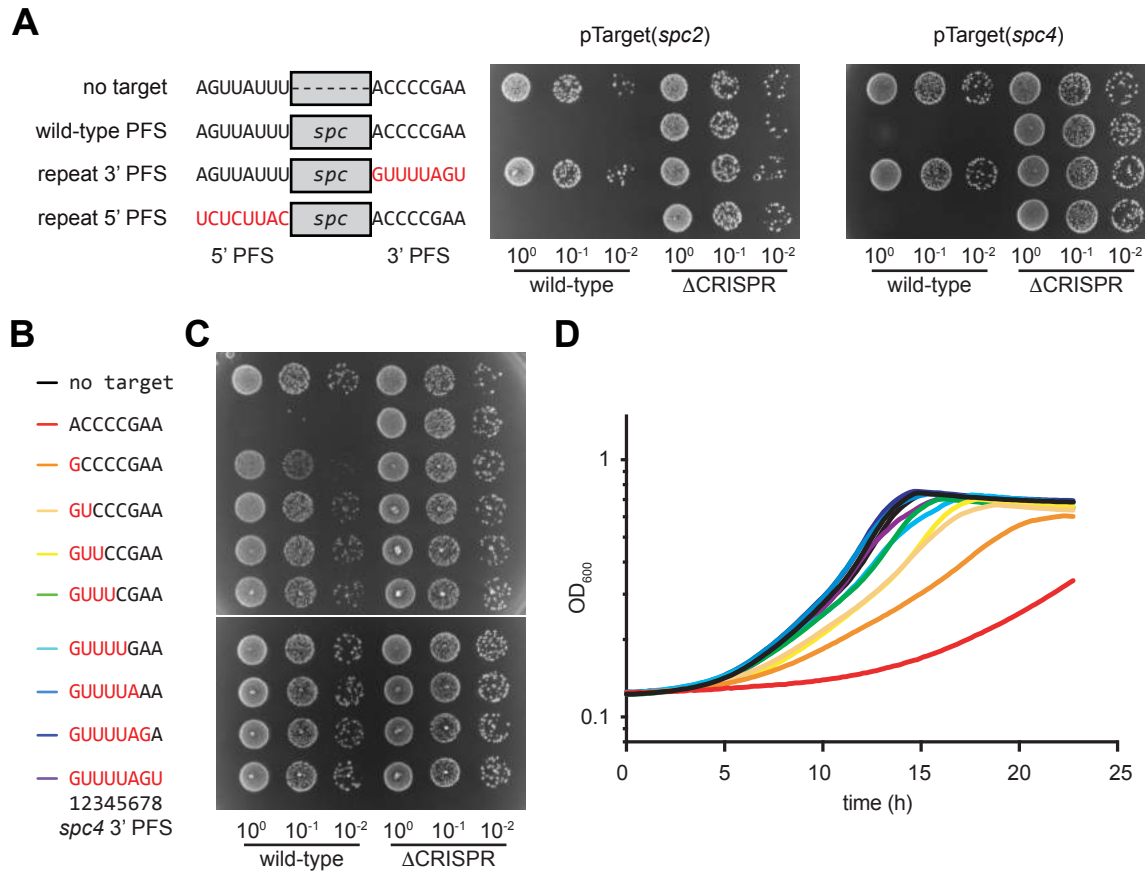


Figure S3: Repeat-like sequences on 3' end of the protospacer confer protection from type VI CRISPR targeting, related to Fig 4. A. Conjugation assay showing 8nt of repeat-like sequence on the 3' end (but not the 5' end) of the protospacer (*spc2* or *spc4*) confers protection from targeting. **B.** Series of *spc4* pTarget plasmids containing repeat-derived sequences (shown in red) were tested for type VI CRISPR interference using conjugation assay and (D) liquid growth assay. Traces represent the mean from four biological replicates.

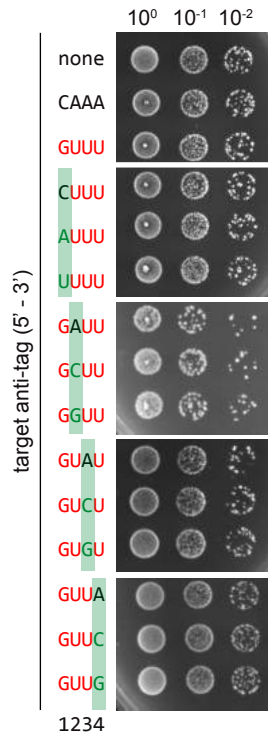


Figure S4: Target plasmid stability in Δ CRISPR strain, related to Fig. 5. Conjugation of pTarget plasmids from Fig 5 into Δ CRISPR strain. Each plasmid contains a mutation in the anti-tag region highlighted in green.

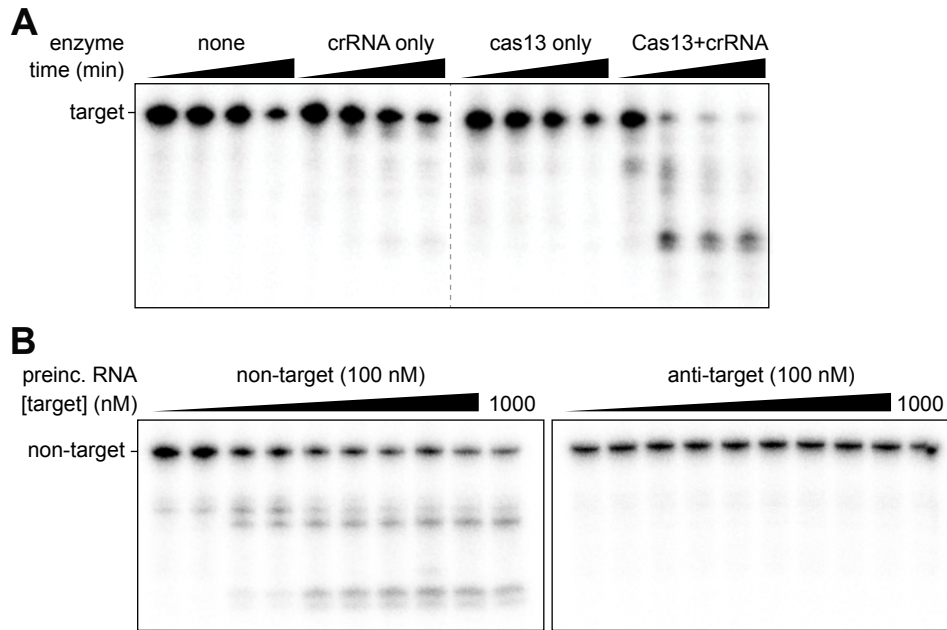


Figure S5: In vitro RNA cleavage assays with LbuCas13 and cleavage inhibition by anti-target RNA, related to Fig. 6. A. *In vitro* RNA cleavage time course with purified LbuCas13 and labeled RNA targets. The indicated RNA substrates were incubated with the Cas13 and / or crRNA and cleavage products analyzed by SDS-PAGE. **B.** Inhibition of *trans*-RNA cleavage by anti-target RNA. 10 nM LbuCas13, 10 nM crRNA, and 10 nM labeled nontarget RNA were incubated with 100 nM nontarget RNA or anti-target RNA. Reactions were initiated with target RNA at 0.05, 0.1, 0.5, 1, 5, 10, 50, 100, 500, or 1000 nM and cleavage products analyzed after 60 minutes.

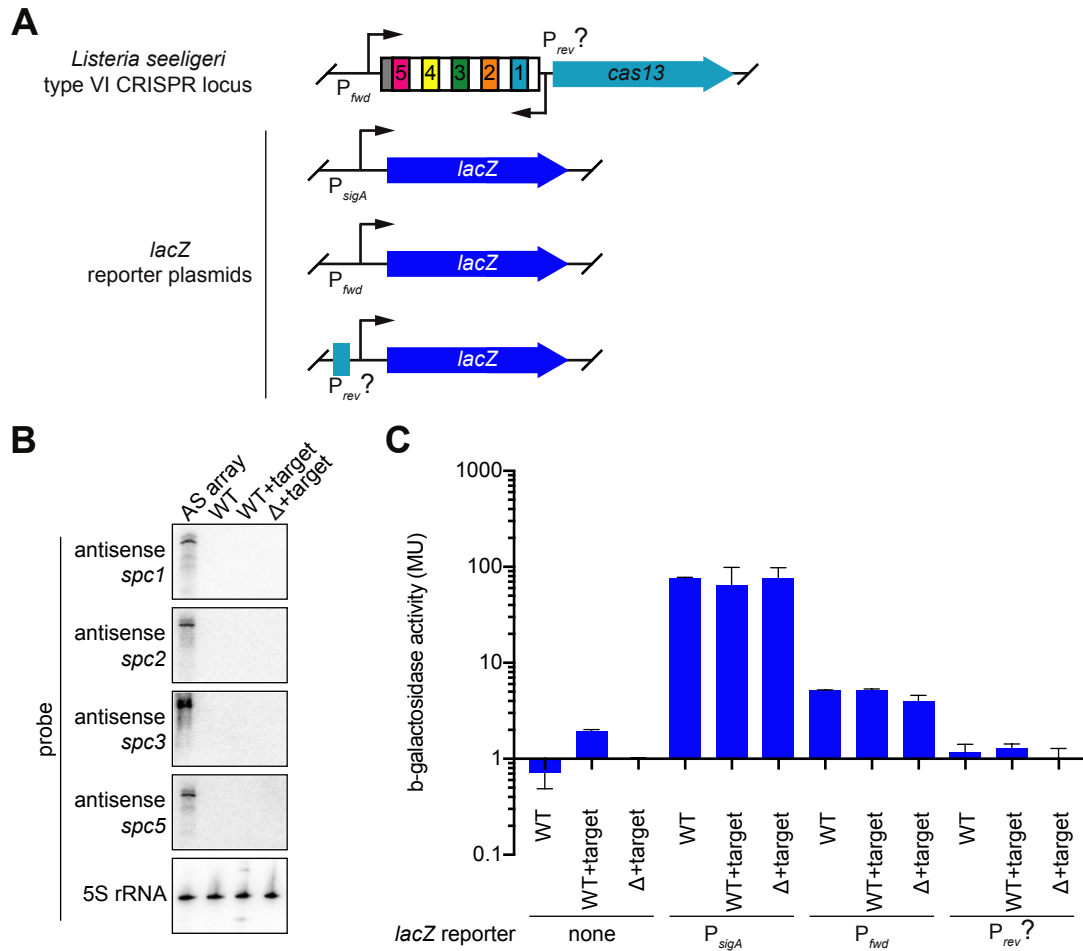


Figure S6: Antisense CRISPR array transcripts are not produced in vivo, related to Figure 7. A. LacZ reporter constructs used to assess antisense transcription from putative promoters downstream of the CRISPR array. A constitutive sigma 70-dependent promoter (P_{sigA}) was fused to *lacZ* as a positive control. Promoters preceding (fwd) and following (rev) the array were tested. **B.** Northern blot analysis using probes against antisense spacer sequences or 5S rRNA loading control in the indicated strains. A strain overexpressing the antisense CRISPR array was analyzed as a positive control. **C.** β -galactosidase assay of the reporters in **A**. Expression from the P_{sigA} , P_{fwd} , and P_{rev} promoters was measured in wild type with and without *spc4* target induction, as well as in the Δ CRISPR strain. Error bars represent standard error of the mean from two biological replicates.